Volume 15 | Number 6 | 21 March 2015 | Pages 1397–1620

Lab on a Chip

Miniaturisation for chemistry, physics, biology, materials science and bioengineering

www.rsc.org/loc

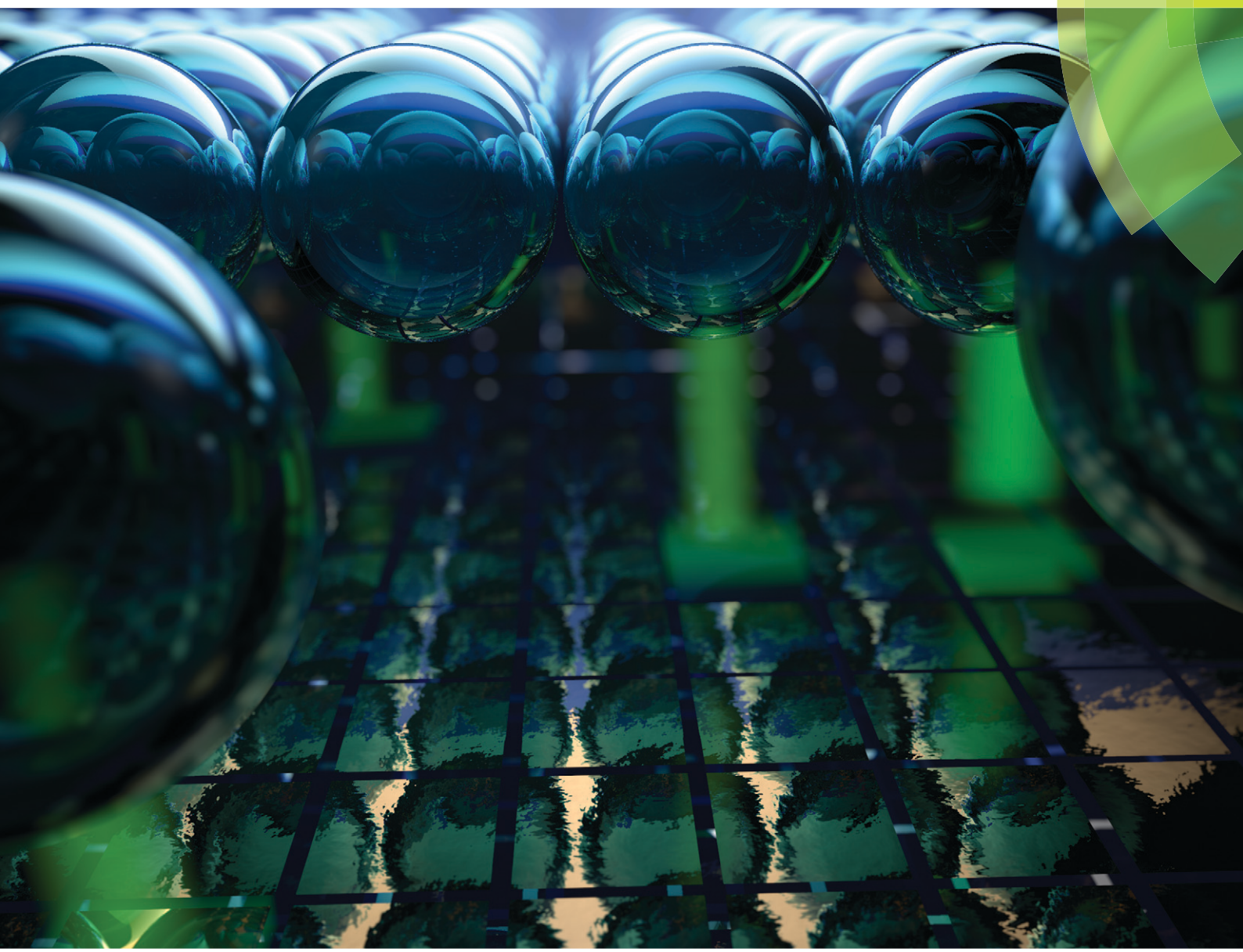

ISSN 1473-0197

ROYAL SOCIETY OF CHEMISTRY

PAPER
Sindy K. Y. Tang *et al.*
Optofluidic ultrahigh-throughput detection of fluorescent drops

Lab on a Chip

PAPER

View Article Online
View Journal | View Issue

Published on 08 January 2015. Downloaded by University of Central Florida on 16/03/2015 19:01:55.

Cite this: *Lab Chip*, 2015, **15**, 1417

Optofluidic ultrahigh-throughput detection of fluorescent drops†

Minkyu Kim,[a] Ming Pan,[b] Ya Gai,[c] Shuo Pang,[d] Chao Han,[e] Changhuei Yang[e] and Sindy K. Y. Tang*[a]

Received 15th December 2014,
Accepted 8th January 2015

DOI: 10.1039/c4lc01465k

www.rsc.org/loc

This paper describes an optofluidic droplet interrogation device capable of counting fluorescent drops at a throughput of 254 000 drops per second. To our knowledge, this rate is the highest interrogation rate published thus far. Our device consists of 16 parallel microfluidic channels bonded directly to a filter-coated two-dimensional Complementary Metal-Oxide-Semiconductor (CMOS) sensor array. Fluorescence signals emitted from the drops are collected by the sensor that forms the bottom of the channel. The proximity of the drops to the sensor facilitates efficient collection of fluorescence emission from the drops, and overcomes the trade-off between light collection efficiency and field of view in conventional microscopy. The interrogation rate of our device is currently limited by the acquisition speed of CMOS sensor, and is expected to increase further as high-speed sensors become increasingly available.

1. Introduction

Droplet microfluidics has enabled a wide range of high throughput screening applications.[1–7] It is now possible to generate and manipulate droplets at kilohertz speeds.[8] In many biochemical assays, fluorescence is used as a read-out for the reactions occurring inside the drops, and can indicate the presence of cells or molecules of interest. In some applications where the sample is compartmentalized at a limiting dilution such that each drop contains one or zero cell or molecule, the number of fluorescent drops directly quantifies the concentration of bacteria present,[4,5] or the amount of DNA mutation.[2] Ability to enumerate fluorescent drops in a high throughput manner is thus advantageous for the rapid detection of various diseases such as sepsis or cancer. The optical detection of fluorescence signal is commonly performed in a serial manner, where drops are injected into a funnel-shaped microchannel consisting of a narrow constriction which forces the drops to arrange in a single file, and to ensure that drops enter the detection region one at a time.[2–6,9,10] We have recently shown that the throughput of the serial interrogation process is limited by the rate at which droplets become unstable and undergo undesirable break-up as they flow through the constriction.[11] To achieve a droplet break-up rate of less than 1%, the maximum throughput was approximately 7000 drops s^{-1} for 40 pL drops. At this rate, it would take 1 hour to interrogate 1 mL (2.5×10^7) of drops, or 40 hours to interrogate 10^9 drops. In previous work, the rate of interrogation actually used was significantly lower than 7000 drops s^{-1}. For example, Pekin *et al.* reinjected 50 pL drops into a funnel-shaped channel at 0.15 mL h^{-1} or 270 drops s^{-1}, for the fluorescence screening of mutant *KRAS* oncogene in genomic DNA.[2]

While multiple droplet generators have been parallelized to increase the throughput of droplet generation at rates up to 320 mL h^{-1} or 189 500 drops s^{-1},[12–15] the serial interrogation process could be a bottleneck limiting the overall throughput of droplet-based assays.[16] The key challenge in performing optical interrogation in a largely parallel manner is the trade-off between light collection efficiency and the field of view which determines the number of drops that can be imaged at a time. To overcome this challenge, on-chip lens arrays have been incorporated to increase light collection efficiency in imaging systems having a large field of view.[17,18] For example, Schonbrun *et al.* aligned a microfabricated zone-plate array with 64 parallel microfluidic channels, and achieved a maximum interrogation throughput of 184 000 drops s^{-1}.[17] The collection efficiency of the zone plate was equivalent to that of an objective lens with a numerical aperture (NA) of 0.48. Lim *et al.* used a microlens array and incorporated mirror surfaces on the bottom of the channel to obtain an NA of 0.51. A throughput of 50 000 drops s^{-1} was

[a] *Department of Mechanical Engineering, Stanford University, CA 94305, USA. E-mail: sindy@stanford.edu*
[b] *Department of Material Science and Engineering, Stanford University, CA 94305, USA*
[c] *Department of Aeronautics and Astronautics, Stanford University, CA 94305, USA*
[d] *College of Optics and Photonics (CREOL), University of Central Florida, FL 32816, USA*
[e] *Department of Electrical Engineering, California Institute of Technology, CA 91125, USA*

† Electronic supplementary information (ESI) available. See DOI: 10.1039/c4lc01465k

Published on 08 January 2015. Downloaded by University of Central Florida on 16/03/2015 19:01:55.

achieved using 25 parallel channels.[18] The key limitations of these two systems are that they require the use of high-speed cameras which are typically costly and not portable. Alternatively, Hatch *et al.* used a 21-megapixel consumer digital single lens reflex (DSLR) camera with a macrolens for wide-field imaging of fluorescent drops.[19] With this design, they imaged over one million drops in a single shot with a resolution of 20–40 pixels per drop. This method required 4–8 seconds of exposure time, however. Assuming the entire chamber of drops could be replenished instantaneously between consecutive shots, the maximum throughput of this approach would be ~125 000–250 000 drops s^{-1}. Also, the numerical aperture of their imaging system was relatively low, with an NA of ~0.089 only.

In this paper, we describe a new approach to overcome the trade-off between light collection efficiency and the throughput of droplet interrogation by integrating microchannels directly on a low-cost CMOS sensor which forms the bottom of the microchannel. Previously, this design has been used in an optofluidic microscope along with Fresnel zone plate array for the fluorescence imaging of cells at a spatial resolution of 1 μm.[20] Since the diameter of drops used in droplet microfluidics applications are typically on the order of tens to hundreds of micrometers, no high resolution imaging is necessary for the enumeration of fluorescent drops. Here we show that it is possible to use a very simple design to count drops containing fluorescein solutions at concentrations of tens of micromolars at a rate of 254 000 drops s^{-1}, the highest interrogation rate published thus far. We also show that our method is capable of quantifying fluorescent drops among non-fluorescent ones at mixture ratios over 4 orders of magnitude from 1 ppm to 5×10^4 ppm, where ppm is defined as the number of fluorescent drops per 10^6 drops.

The key advantages of our method are: i) the proximity of the drops to the sensor facilitates efficient collection of fluorescence from the bottom hemisphere of a drop, which is close to 50% of the total emission. As a reference, a 40× (0.65 NA) microscope objective collects ~12% of the total emission only. ii) The optical system is low-cost and portable as it does not require microscopes, objectives, or high-speed cameras. iii) The use of a wide microfluidic channel allows the drops to be injected at high volumetric flow rates without break-up. Unlike the serial interrogation process, the interrogation rate of our system is not rate-limited by the stability of the drops,[11] but rather, by the speed of the CMOS sensor. Our interrogation rate can thus be further improved as low-cost and high-speed imagers become increasingly available.

2. Experimental design

2.1 Droplet generation

We used methods in soft lithography to fabricate microchannels in poly(dimethylsiloxane) (PDMS).[21] The microchannels were rendered hydrophobic by treatment with Aquapel (Pittsburgh, PA) to avoid droplet wetting of the wall. We generated 40 pL monodisperse droplets using flow-focusing nozzles.[22] The continuous phase was a hydrofluoroether HFE-7500 (3M, St. Paul, MN) containing an ammonium salt of Krytox (2% w/w) as a surfactant to stabilize the drops against coalescence. We collected the drops generated from the flow-focusing nozzles in syringes (Normject 3 mL). As water has a lower density than HFE-7500 does (ρ = 1.63 g mL^{-1}), the drops creamed to the top of the syringes to form a concentrated emulsion after 5 hours of storage. The drops were kept at 4 °C to prevent the evaporation of the liquids. The size of the drops remained unchanged after this storage time. For all experiments, we used concentrated emulsions with volume fraction φ = 85.6 ± 3.1%. Different volumes of fluorescent "positive" drops were pipetted and mixed with empty "negative" drops containing buffer only to obtain different concentrations of positive drops. This mixture of drops was reinjected into a microchannel at fixed volumetric flow using a syringe pump (Kent Scientific). The channel had a height of 36 μm, less than one droplet diameter, and the drops flowed as a 2D monolayer.

2.2 Integration of microfluidics on CMOS sensor and optical setup

We used a CMOS sensor (Aptina, MT9M001) consisting of 1280 × 1024 pixels, each pixel having a size of 5.2 μm. We removed the glass cover, and spin-coated a band-pass filter to block the transmission of excitation light (see Note S1† for details). The filter was a photoresist-based material containing a green filter pigment (provided by Fuji Film, Part# SG-5001L). The transmission spectrum of the filter material is included in Fig. S1.† The filter, having a thickness of about 6 μm, provided an optical density (OD) difference of about 3 between 488 nm (excitation wavelength) and 520 nm (emission wavelength). This OD difference was sufficient for the detection of 10 μM fluorescein drops in a channel with a height of 36 μm. For the imaging of decreased concentrations of fluorophores, the number of layers of filters can be increased to further increase the OD difference. A thin layer (~1 μm) of PDMS was then spin-coated on this filter. The top PDMS channel was bonded to this surface after oxidation with oxygen plasma (Fig. 1a).

We used a blue LED (250 mW, peak emission at 490 nm, Thorlabs Part# M490L3) to excite fluorescence in the drops. An excitation filter (Semrock, Part#, FF01-475/35-25) was used to block light below 457.5 nm and above 492.5 nm. The emitted light from the fluorescent drops was collected on the CMOS sensor. Fig. 1b shows the optical setup. A custom MATLAB GUI that interfaced with the imaging software (EPIX, XCAP) was used to acquire images on the CMOS sensor. Data processing was performed subsequently using a custom script in MATLAB.

3. Results and discussions

3.1 Parallel droplet interrogation rate

Since the drops were monodisperse with known size, volume fraction and velocity profile in the channels (see Fig. 1d), it

 This journal is © The Royal Society of Chemistry 2015

Published on 08 January 2015. Downloaded by University of Central Florida on 16/03/2015 19:01:55.

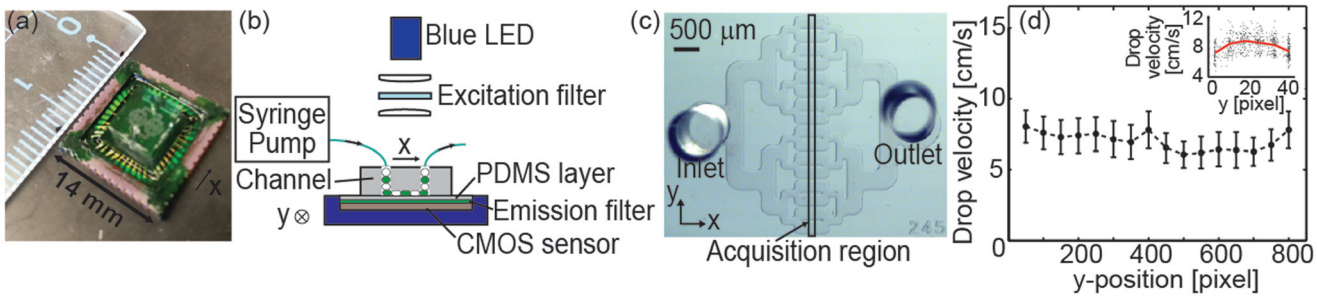

Fig. 1 a) Photograph of the device consisting of a microchannel bonded directly on a CMOS sensor. b) Experimental setup for characterizing the device. c) Photograph of microchannel used. The optical acquisition region is indicated in the black box (see text). d) Droplet velocity profile in the acquisition region. The error bar represents one standard deviation from the mean. The volumetric flow rate Q of the emulsion was Q = 43 mL h^{-1} which corresponds to 254 000 drops per second. The inset shows droplet velocity profile in one of the 16 channels. One channel is about 6 droplet diameters wide. The red line connects the mean droplet velocity at the centroid location of these 6 drops.

was possible to interrogate the drops with a simple detection scheme by counting the number of fluorescent blobs that passed through a given region of the CMOS sensor. Although the sensor array was two-dimensional, we acquired data only from a central strip of pixels ($\Delta x \times \Delta y$ = 4 × 852 pixels) aligned perpendicular to the direction of flow of the drops. Fig. 1c indicates this acquisition region. The use of this 4 pixel-wide region allowed us to operate the CMOS at the maximum acquisition rate of the sensor at 2125 fps. Using a narrower strip of pixels did not increase the acquisition rate in this sensor. We could not use the entire height of the sensor (1280 pixels) as space was needed to bond the side wall of the PDMS channel to the sensor. We note that a linear photosensor array would suffice for our simple detection scheme here. It would have been difficult to bond a wide PDMS channel to a linear sensor array without extra steps of planarization, however. We have thus chosen to use a 2D sensor array to facilitate the bonding and integration with the PDMS channel.

At a CMOS acquisition rate of 2125 fps, the maximum speed the drops (diameter ~40 μm) can flow was about 8.5 cm s^{-1}, beyond which the signal would be under-sampled, *i.e.*, a fluorescent drop may pass the 4 pixel-wide acquisition region in less than one frame and cannot be detected. At an average flow speed of 8.5 cm s^{-1}, the equivalent volumetric flow rate of the emulsion was 43 mL h^{-1} (for a droplet volume of 40 pL and a volume fraction of 85%) and the equivalent throughput we obtained was 254 000 drops s^{-1}. Table S1† shows the expected droplet interrogation rate as a function of drop size, assuming that only a monolayer of drops is imaged at a time. Here, the droplet interrogation rate was limited by the speed of the CMOS, rather than the stability of the drops since no narrow constrictions were involved and the operating capillary number in our system was about 0.005, lower than that required for droplet breakup.[11,23]

Fig. 1c shows the geometry of the channel we used. It consisted of 16 parallel microfluidic channels each having a width of 245 μm or 6–7 droplet diameters. We have chosen such channel geometry to obtain a plug-like velocity profile of all drops as they flow through the acquisition region on the CMOS sensor (Fig. 1d). Although the use of a single wide channel would increase the space that can be filled by the drops (instead of PDMS channel walls in the case of 16 channels), the large variation in velocity from the center of the channel to the edge of the channel led to a decreased overall droplet interrogation rate (see Fig. S2 and Table S2†). Since our maximum droplet interrogation rate was limited by the CMOS sensor, its acquisition rate set the upper limit of droplet speed in the center of the channel where the drops were flowing the fastest. As the drops by the wall had a velocity close to zero, the pixels in those regions were not utilized at their maximum acquisition capacity. We estimated the maximum droplet interrogation rate to be ~100 000 drops s^{-1} only, less than half of the rate we achieved with the 16-channel design.

3.2 Optical characterization

To characterize the optical sensitivity of our device, we injected the emulsion into the channel and stopped the flow. Fig. 2a shows an image of the emulsion without flow, where only 12 fluorescent drops were visible as bright blobs, as acquired by the CMOS sensor in a region of size 400 × 425 pixels. The intensity profile of a single fluorescent drop is shown in Fig. 2b. This profile matched well with our calculation based on the divergence of light from a drop which we approximated as a collection of point sources (see Note S2†).

Fig. 2c shows the signal-to-noise ratio (SNR) of fluorescence measurements using our device as a function of the concentration of fluorescein which we used as a model fluorophore. We defined the SNR to be the measured peak intensity of a fluorescent drop to the mean intensity of the non-fluorescent background consisting of negative drops and the continuous phase. The lowest concentration of fluorescein we attempted to measure from the drops in a 36 μm-tall channel was 5 μM, which gave a SNR of 2. The ability to detect 5 μM of fluorophore solution was sufficient for enzymatic assays involving the use of fluorogenic substrates, which are often used at relatively high concentrations above 20 μM.[24,25] While out of scope of the current work, existing methods can

Published on 08 January 2015. Downloaded by University of Central Florida on 16/03/2015 19:01:55.

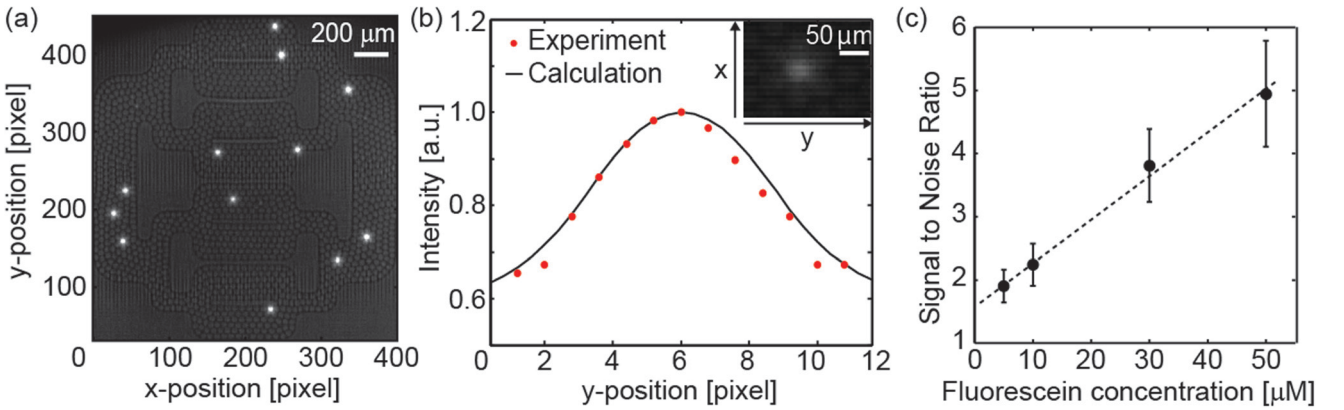

Fig. 2 a) Image of our emulsion consisting of a mixture of positive (fluorescent) drops containing a 10 μM solution of fluorescein and negative drops containing buffer only, as acquired by our CMOS sensor. The contrast of the image has been increased to facilitate visualization of the fluorescent drops. The drops have a volume of 40 pL and the volume fraction of the emulsion was about 85%. b) Intensity profile of a fluorescent drop measured by our CMOS sensor. The data (red markers) is consistent with the calculated intensity profile (black line). The inset shows an image of the fluorescent drop. c) The measured signal to noise ratio as a function of fluorescein concentration.

be applied to increase the SNR of fluorescence detection, such as by incorporating lens arrays to focus the excitation light onto the drops,[17,20] by using filter materials with higher rejection ratio between the excitation and emission wavelengths, by using a stronger light source, or by introducing spatial modulation methods.[26]

3.3 Accuracy and dynamic range of droplet interrogation

To interrogate an increased number of drops, a continuous flow was applied to the drops and the sensor was set to record intensity values within the acquisition region (4 × 852 pixels) over a finite number (10^4–10^5) of frames at 2125 fps. Fig. 3a shows a kymograph of the imaged emulsion from the acquisition region over 100 frames or 47 milliseconds. The raw intensity data within the acquisition region from all frames were stacked laterally to generate the kymograph, where the vertical axis is the *y*-position in the acquisition region, the horizontal axis is frame number or time, and the color represents the measured intensity value (Fig. 3a). In this kymograph, the height of the bright spot or "blob" represents the imaged diameter of a fluorescent drop (assuming the drop is isolated from other fluorescent drops), while the length of the blob represents the residence time of the drop in the acquisition region. We used a simple thresholding by intensity in MATLAB to digitize the kymograph (Fig. 3b), *i.e.*, regions with intensity above (or below) a certain threshold will be given a value of 1 (or 0). The number of regions with a value of 1 (referred to as "digitized blobs") was then used to derive the number of fluorescent drops present in the emulsion. As multiple fluorescent drops could be in contact with each other and our MATLAB image analysis would recognize them as a single blob, the number of digitized blobs would be smaller than the number of fluorescent drops actually present. It is, in principle, possible to use the intensity distribution within a blob to derive the number of fluorescent drops in direct contact with each other. Such derivation is possible since the resulting intensity profile is a simple superposition of the intensity profiles of individual drops (Fig. S3a†). This method works well as long as the intensity profiles from all drops are identical, which requires: i) the excitation source is uniform across the entire acquisition region, ii) the concentration of the fluorophore is identical in all drops, and iii) all drops move at the same speed (slow-moving drops would appear longer and larger). None of the above three requirements were satisfied in our experiments, however. This fact was indirectly reflected in the wide size distribution of the digitized blobs (Fig. S4†): if the intensity profile from all drops were identical, we would expect a narrow distribution of blob sizes at discrete locations that correspond to one drop, or two drops in contact. Instead, we obtained a wide, continuous distribution of blob sizes. Such wide distribution originated from the non-uniformity of excitation light source and the velocity fluctuation of the drops. The standard deviation in droplet velocity in our system was about 20% (Fig. S5a†). At a fixed location in the channel, the lowest droplet velocity measured was up to two times less than the highest droplet velocity measured (Fig. S5b†). Such slow-moving drops appeared two times bigger than the fast-moving drops. While it is possible to calibrate for the non-uniformity of the excitation source and the error originating from the variations in droplet speed, it is impossible to account for the non-uniform fluorophore concentrations which will vary in actual applications.

As such, we use a different method to extract the expected number of fluorescent drops by calculating the probability that more than one drop would be in direct contact. Previously, the Poisson probability of more than one molecule being encapsulated into a single drop has been used to derive the expected number of genes from the measured number of fluorescent drops.[2] For a given fluorescent ("positive") drop in a hexagonal packing, we approximate the probability P_1 that it is surrounded by six non-fluorescent ("negative") drops by eqn (1):

 This journal is © The Royal Society of Chemistry 2015

Published on 08 January 2015. Downloaded by University of Central Florida on 16/03/2015 19:01:55.

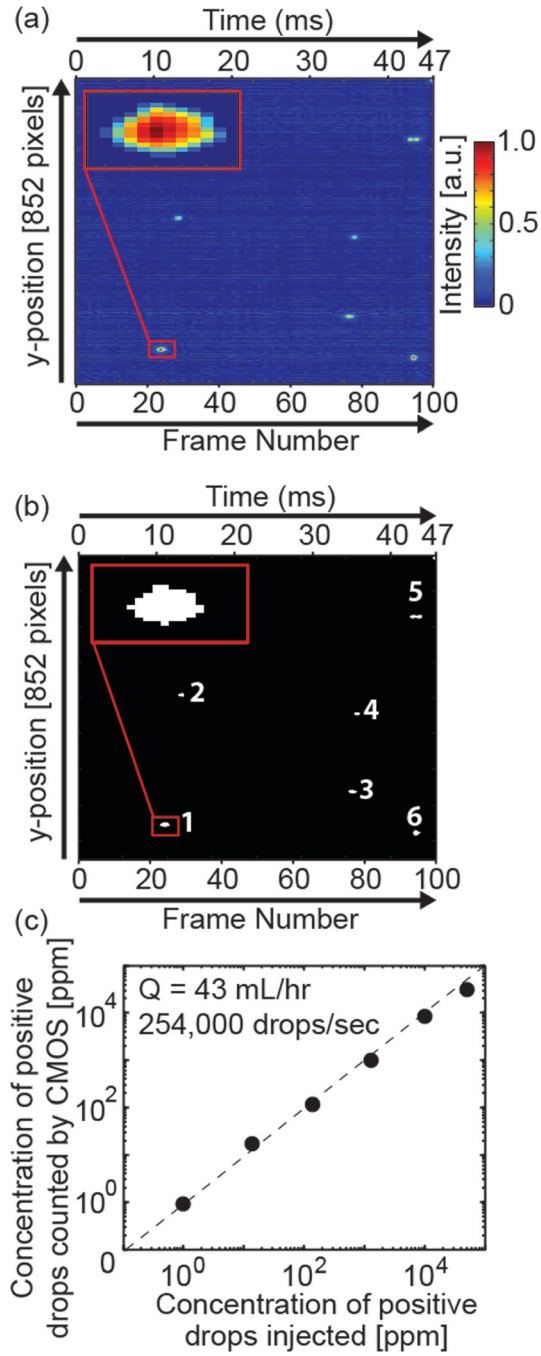

Fig. 3 a) A kymograph of positive drops acquired by the CMOS sensor. This kymograph was constructed from a sequence of 100 frames (corresponding to 47 ms) stacked laterally. b) Digitized kymograph where fluorescent blobs are identified as regions with intensity above a certain threshold value. Insets show the zoomed-in kymograph and digitized image of blob 1, as indicated in the red boxes and a) and b), respectively. c) Linearity and dynamic range of our detection method. The experiment was performed at a flow rate of 43 mL h^{-1}.

$$P_1 = (C_-)^6 = (1 - C_+)^6 \quad (1)$$

where C_+ and C_- are the concentrations of positive and negative drops respectively. The probability P_{multi} that a given positive drop is in direct contact with more than one positive drop is then given by eqn (2).

$$P_{\text{multi}} = 1 - (1 - C_+)^6 \quad (2)$$

Here we ignore the next nearest neighbors and beyond that might be fluorescent leading to three or more drops in contact, as these cases are increasingly unlikely for low concentrations of fluorescent drops, a regime we target our device towards. Based on the probability P_{multi}, we can then derive the expected concentration of fluorescent positive drops C_+ from the measured number of blobs N_{blob} and the total number of drops in the emulsion N_{tot} (see note S3 and S4† for derivations):

$$C_+ \approx \frac{1}{6}\left(1 - \sqrt{1 - 12\frac{N_{\text{blob}}}{N_{\text{tot}}}}\right) \quad (3)$$

The advantage of using this correction scheme based on the probability of drops in contact is that it does not require the use of the size or the intensity profile of the detected blobs. It should be less prone to errors due to non-uniformity in excitation source intensity, velocity variations in the drops,

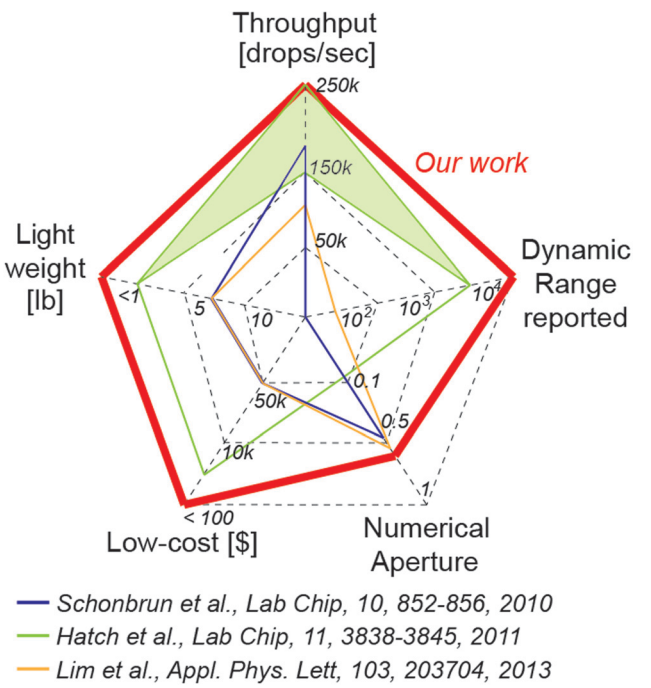

Fig. 4 Comparison of our work with selected prior work. As a note, the droplet volumes used in our work, Schonbrun's, Hatch's and Lim's are 40 pL, 4 pL, 50 pL, and 100 pL respectively. For the throughput in Hatch *et al.*, a range is given assuming an exposure time of 4–8 seconds and instantaneous replenishment of drops between shots (see text). The dynamic range is the range of concentration of positive drops (C_+ in text) detected in prior work and this work. If we account for the loss in transmission in the filter layer, we estimated the effective NA of our system to be about 0.6. The cost and weight of the systems are estimated for the imager (*e.g.*, high-speed camera) only excluding other optics such as the light source.

Published on 08 January 2015. Downloaded by University of Central Florida on 16/03/2015 19:01:55.

and other errors that cause unknown changes in the detected droplet intensity profile.

Fig. 3c shows that our interrogation method can be applied to measure positive droplet concentrations (C_+) over 4 orders of magnitude from 1 ppm to 5×10^4 ppm, where ppm is defined as the number of fluorescent drops per 10^6 drops. The slight deviations between the values of C_+ measured and that injected are likely due to the inaccurate manual procedure of preparing emulsion mixtures and the inhomogeneous mixing of positive and negative drops within the emulsion. In addition, the deviation of the data point at $C_+ = 5 \times 10^4$ ppm is expected: our method ignored cases where three or more fluorescent drops were in contact, which was not entirely valid for high values of C_+ (see Note S4 and Table S3†). However, for $C_+ < 10^4$ ppm, the probability of more than two fluorescent drops in contact is low (Table S3†). The number of detected blobs will eventually converge with the actual number of positive drops at very low values of C_+. Our method is thus increasingly accurate as the concentration of positive drops decreases.

4. Conclusions

We have described a simple method for the ultrahigh-throughput parallel interrogation of drops directly on an optofluidic CMOS platform. Fig. 4 shows a spider-web comparison of our work with a few methods described previously. As not all quantities were reported in prior work, we have made rough approximations in constructing the chart. As can be seen, our method has multiple advantages over existing systems in terms of throughput, dynamic range, cost and portability. While the sensitivity of our method is not ideal, ongoing work is in progress to apply existing methods to increase the SNR of fluorescence detection. Finally, we note that as CMOS sensors with acquisition rates over 10 million per second have been reported,[27–29] our method has the additional advantage that it can leverage the increasing availability of such ultrahigh-speed sensors to achieve further increase in the interrogation rate of droplets without having to re-engineer the design of our current system.

Acknowledgements

We acknowledge Fengjiao Lyu for helpful discussions and assistance with initial experiments. We also acknowledge partial support from the California Sea Grant College Program (CASG), the Stanford Woods Institute for the Environment, Stanford Nano Shared Facilities Bio/Medical Mini Seed Grant, and the Stanford Center for Innovation in Global Health. ST acknowledges additional support from the 3M Non-tenured Faculty Award.

References

1 M. M. Kiss, L. Ortoleva-Donnelly, N. R. Beer, J. Warner, C. G. Bailey, B. W. Colston, J. M. Rothberg, D. R. Link and J. H. Leamon, *Anal. Chem.*, 2008, **80**, 8975–8981.
2 D. Pekin, Y. Skhiri, J. C. Baret, D. Le Corre, L. Mazutis, C. B. Salem, F. Millot, A. El Harrak, J. B. Hutchison, J. W. Larson, D. R. Link, P. Laurent-Puig, A. D. Griffiths and V. Taly, *Lab Chip*, 2011, **11**, 2156–2166.
3 J. J. Agresti, E. Antipov, A. R. Abate, K. Ahn, A. C. Rowat, J.-C. Baret, M. Marquez, A. M. Klibanov, A. D. Griffiths and D. A. Weitz, *Proc. Natl. Acad. Sci. U. S. A.*, 2010, **107**, 4004–4009.
4 J. Q. Boedicker, L. Li, T. R. Kline and R. F. Ismagilov, *Lab Chip*, 2008, **8**, 1265–1272.
5 K. Churski, T. S. Kaminski, S. Jakiela, W. Kamysz, W. Baranska-Rybak, D. B. Weibel and P. Garstecki, *Lab Chip*, 2012, **12**, 1629–1637.
6 E. Brouzes, M. Medkova, N. Savenelli, D. Marran, M. Twardowski, J. B. Hutchison, J. M. Rothberg, D. R. Link, N. Perrimon and M. L. Samuels, *Proc. Natl. Acad. Sci. U. S. A.*, 2009, **106**, 14195–14200.
7 L. Mazutis, A. F. Araghi, O. J. Miller, J.-C. Baret, L. Frenz, A. Janoshazi, V. Taly, B. J. Miller, J. B. Hutchison, D. Link, A. D. Griffiths and M. Ryckelynck, *Anal. Chem.*, 2009, **81**, 4813–4821.
8 M. T. Guo, A. Rotem, J. A. Heyman and D. A. Weitz, *Lab Chip*, 2012, **12**, 2146–2155.
9 B. Kintses, L. D. van Vliet, S. R. A. Devenish and F. Hollfelder, *Curr. Opin. Chem. Biol.*, 2010, **14**, 548–555.
10 A. B. Theberge, F. Courtois, Y. Schaerli, M. Fischlechner, C. Abell, F. Hollfelder and W. T. S. Huck, *Angew. Chem., Int. Ed.*, 2010, **49**, 5846–5868.
11 L. Rosenfeld, L. Fan, Y. Chen, R. Swoboda and S. K. Y. Tang, *Soft Matter*, 2014, **10**, 421–430.
12 W. Li, J. Greener, D. Voicu and E. Kumacheva, *Lab Chip*, 2009, **9**, 2715–2721.
13 M. B. Romanowsky, A. R. Abate, A. Rotem, C. Holtze and D. A. Weitz, *Lab Chip*, 2012, **12**, 802–807.
14 T. Nisisako, T. Ando and T. Hatsuzawa, *Lab Chip*, 2012, **12**, 3426–3435.
15 T. Nisisako and T. Torii, *Lab Chip*, 2008, **8**, 287–293.
16 L. Rosenfeld, T. Lin, R. Derda and S. K. Y. Tang, *Microfluid. Nanofluid.*, 2014, **16**, 921–939.
17 E. Schonbrun, A. R. Abate, P. E. Steinvurzel, D. A. Weitz and K. B. Crozier, *Lab Chip*, 2010, **10**, 852–856.
18 J. Lim, P. Gruner, M. Konrad and J.-C. Baret, *Lab Chip*, 2013, **13**, 1472–1475.
19 A. C. Hatch, J. S. Fisher, A. R. Tovar, A. T. Hsieh, R. Lin, S. L. Pentoney, D. L. Yang and A. P. Lee, *Lab Chip*, 2011, **11**, 3838–3845.
20 S. Pang, C. Han, L. M. Lee and C. Yang, *Lab Chip*, 2011, **11**, 3698–3702.
21 Y. N. Xia and G. M. Whitesides, *Annu. Rev. Mater. Sci.*, 1998, **28**, 153–184.
22 S. L. Anna, N. Bontoux and H. A. Stone, *Appl. Phys. Lett.*, 2003, **82**, 364–366.
23 G. F. Christopher, J. Bergstein, N. B. End, M. Poon, C. Nguyen and S. L. Anna, *Lab Chip*, 2009, **9**, 1102–1109.
24 H. Xie, J. Mire, Y. Kong, M. Chang, H. A. Hassounah, C. N. Thornton, J. C. Sacchettini, J. D. Cirillo and J. Rao, *Nat. Chem.*, 2012, **4**, 802–809.

 This journal is © The Royal Society of Chemistry 2015

25 J. Lim, J. Vrignon, P. Gruner, C. S. Karamitros, M. Konrad and J.-C. Baret, *Appl. Phys. Lett.*, 2013, **103**, 203704.
26 P. Kiesel, M. Bassler, M. Beck and N. Johnson, *Appl. Phys. Lett.*, 2009, **94**, 041107.
27 M. El-Desouki, M. J. Deen, Q. Fang, L. Liu, F. Tse and D. Armstrong, *Sensors*, 2009, **9**, 430–444.
28 T. G. Etoh, D. V. T. Son, T. Yamada and E. Charbon, *Sensors*, 2013, **13**, 4640–4658.
29 Y. Kondo, K. Takubo, H. Tominaga, R. Hirose, N. Tokuoka, Y. Kawaguchi, Y. Takaie, F. Yano, T. Daigen, A. Ozaki and S. Nakaya, *Shimadzu Hyoron*, 2012, **69**, 285–291.

Published on 08 January 2015. Downloaded by University of Central Florida on 16/03/2015 19:01:55.